ROYAL SOCIETY
OF CHEMISTRY

## PAPER

Check for updates

# Influence of reactive oxygen species concentration and ambient temperature on the evolution of chemical bonds during plasma cleaning: a molecular dynamics simulation

Yuhai Li, [ID] [ab] Yilan Jiang,[b] Xujie Liu,[a] Qingshun Bai, [ID] *[a] Hao Liu,[b] Jingxuan Wang,*[b] Peng Zhang,*[ac] Lihua Lu[a] and Xiaodong Yuan[b]

The research on plasma chemistry involved in the formation and dissociation of abundant chemical bonds is fundamental to developing plasma cleaning. To understand the influence of reactive oxygen species' concentration and ambient temperature on the evolution behavior of the chemical bond during plasma cleaning, microscopic reaction models between organic contaminants and reactive oxygen species were established and performed by reactive molecular dynamics. Dibutyl phthalate, as a representative organic contaminant, was selected as the research object. The simulation results suggested that hydrogen bonds between hydroxyl radicals reduced the mobility of reactive species, resulting in the cleaning ability of hydroxyl radicals being much lower than atomic oxygen and ozone radicals. The concentration of reactive species dominated the efficiency of plasma cleaning, and the increase in ambient temperature further improved the cleaning ability. C–H, C–C and C–O bonds were gradually oxidized to C=C, C–O, C=O and O–H bonds by hydrogen abstraction reaction during the reaction of reactive species with organic contaminants. An increase in ambient temperature induced the possibility of benzene ring destruction under the action of reactive species, which was considered a method of complete dissociation of aromatic hydrocarbons.

## 1 Introduction

Organic contaminants can significantly degrade the physical properties and the interfacial performance of materials.[1–4] Materials are inevitably contaminated by hydrocarbons in manufacturing, transportation and installation, which need to be cleaned thoroughly before serving. Besides, components must be dissembled for cleaning after long service, especially in an ambient vacuum.[5] Currently, routine cleaning methods such as chemical solution, UV–ozone, laser and carbon dioxide snow are used to eliminate organic contaminants on the surfaces of components, yet these cleaning methods cause damage and secondary contamination to precision components (*e.g.*, semiconductors and coated optical components).[6–9] Plasma cleaning, as a precision cleaning method, has a broad application in the pretreatment of materials bonding, printing, painting, coating, and etching, complementing conventional cleaning methods.[10–14] Plasma cleaning has the advantages of high

efficiency, environmental friendliness, no secondary contamination, low process cost, and can achieve large area *in situ* cleaning.[4,15] The plasma can also modify the physicochemical nature of surfaces while cleaning surfaces, enhancing surface adhesion strength.[13,16] Thus, plasma cleaning technology has developed into a mature commercial cleaning technology widely employed in the electronics industry, medical treatment, optics, biological materials, polymers, solar cells, and other fields.[17]

The research on low-temperature plasma chemistry is the basis of plasma diagnosis, cleaning, and modification. In plasma treatment, the chemical reaction between hydrocarbon and reactive species plays a leading role, and physical bombardment facilitates the completion of this reaction process at extreme times.[18] Based on the optical diagnosis, it is found that the plasma generates abundant neutral reactive oxygen species (ROS; *e.g.*, O, OH, $O_3$, $HO_2$, $H_2O_2$) and reactive nitrogen species (RNS; *e.g.*, N, NO, $N_2$), and their concentration are sensitive to the type of gas source and discharge parameters.[19–22] According to the detection of elements and chemical bonds, the primary chemical bonds (*e.g.*, C–H, C–C) of organic contaminants are gradually destroyed by reactive oxygen species into small molecular radicals (*e.g.*, CO, $CO_2$, $H_2O$), which desorb from the surface due to the weak

*[a]School of Mechatronics Engineering, Harbin Institute of Technology, Harbin 150000, China. E-mail: qshbai@hit.edu.cn*

*[b]Laser Fusion Research Center, China Academy of Engineering Physics, Mianyang 621900, China. E-mail: wjxsdu@foxmail.com*

*[c]Chongqing Research Institute, Harbin Institute of Technology, Chongqing 401135, China. E-mail: zp@hit.edu.cn*

interatomic forces.[23,24] Normand *et al.*[25] calculated and measured the concentration of long-lived reactive species during the treatment of polymers by oxygen plasma and pointed out that the concentration of neutral reactive species in plasma depends on plasma type and operating pressure. An increase in the concentration of reactive species significantly promotes bond cleavage in hydrocarbons and improves cleaning efficiency, but the concentration of reactive species has a saturation value. Park *et al.*[26] used *in situ* optical absorption spectroscopy to measure the concentrations of ozone and nitrogen oxides in air plasma and revealed the dependence of the chemical properties of the air plasma system on ambient temperature (298 K to 523 K). The generation of type and concentration of reactive species are sensitive to the ambient temperature during gas discharge.[25–28] In addition, during etching parylene-N with oxygen plasma, Russell *et al.*[29] found that the relative content of carbon in aromatic hydrocarbons significantly decreased with the increase in substrate temperature (373 K to 523 K), which provided a new method for dissociating aromatic hydrocarbon contaminants. Samaei *et al.*[30] and Li *et al.*[31] adopted the finite element method to establish a comprehensive physical model for atmospheric and low-pressure plasma cleaning of organic contaminants to predict the removal rate of contaminants. Nevertheless, the effects of reactive species in plasma and their concentration and ambient temperature on removing organic contaminants are still unclear at the atomic level.

However, due to the limitation of experimental equipment, the chemical bond evolution process in the plasma cleaning process cannot be detected and identified. With the development of computational chemistry simulation, molecular dynamics (MD) simulation based on the reactive force field (ReaxFF) is a potential tool to explore the mechanism of plasma cleaning from a microscopic point of view.[32,34] Reactive molecular dynamics (RMD) can accurately describe the chemical bond evolution of hydrocarbon compounds by reactive species in plasma, verified by experimental and simulational studies.[35] Cui *et al.*[36] and Tian *et al.*[37] adopted reactive molecular dynamics to elucidate the reaction pathway of the destruction of biomolecules and the formation of new radicals under the action of reactive oxygen species in the plasma. The simulation results illustrated that OH concentration had an essential effect on the destruction pathway and reaction rate of biomolecules. The authors adopted various experimental characterization methods and reactive molecular dynamics simulations to reveal the microscopic mechanism of low-pressure plasma cleaning of organic contaminants.[38] The evolution of chemical bonds and the main products obtained by the ReaxFF data are consistent with the X-ray photoelectron spectroscopy (XPS) measurement results during plasma cleaning experiments. In addition, methods to explore chemical reaction pathways using ReaxFF have been reported, including degradation of pesticides,[35] medicine,[37] sterilization,[39] *etc.* The microscopic mechanism of interaction between organic molecules and reactive species is revealed by RMD, which provides the theoretical basis for applying low-temperature plasma. Therefore, these study achievements demonstrate that MD can be considered an

effective computational method for studying the microscopic mechanism of chemical reactions in the plasma cleaning process and describing the interaction between organic contaminants and reactive species.

Motivated by this research, this work aims to reveal the chemical reaction mechanism of plasma cleaning based on the ReaxFF molecule dynamic at the atomic level. The effect of ambient temperature, reactive species and their concentration on plasma cleaning ability was discussed. According to simulation results, the main reaction pathway and chemical evolution characteristics were clarified during plasma cleaning, which provides an understanding and accurate control for applying plasma cleaning in the industrial field.

## 2 Models and methodology

### 2.1 Simulation models

It is essential to establish accurate models of interaction between organic contaminants and reactive species in plasma to elucidate the mechanism of plasma cleaning. Firstly, the reactive species in low-pressure air plasma were diagnosed by optical emission spectrometry (OES, Maya 2000 pro), as shown in Fig. 1a. More detailed information about low-pressure air plasma equipment could be found in our previous work.[4] The signals of molecular nitrogen ($N_2$), atomic nitrogen (N I, 821.6 nm), and atomic oxygen (O I, 777.9 nm and 844.6 nm) were found in spectra within 730–850 nm. Among them, atomic oxygen is an important component of reactive oxygen species. The peak intensity of OES spectra has a positive relationship with the concentration of reactive species.[19,20,40] The results show that the concentration of reactive species is sensitive to the operating pressure, which is consistent with Normand's research.[25] These results provide a reference to establish simulation models.

In reality, plasma-excited reactive species penetrate organic films adsorbed on the surface and undergo chemical reactions, as shown in Fig. 1b. Due to the limitation of simulation computing ability, we only simulate the reaction between reactive species and organic contaminants in this work without considering the influence of the substrate on organic contaminants. All simulations in this work were performed in Materials Studio 8.0 software, which can calculate the chemical bond breakage and generation based on the ReaxFF.[39] Unfortunately, this force field cannot support the calculation, limiting the simulation of reactive nitrogen species. Besides, the dibutyl phthalate (DBP) molecule is a common plasticizer that represents most contaminants' chemical properties and can be found on the surface of a wide range of materials.[9,41] Fig. 1c shows the molecular structure of DBP. We chose five DBP molecules and different numbers (20, 40, 80, 120, 160, 200) of reactive oxygen species (ROS; *e.g.*, O, OH, $O_3$, $HO_2$, $H_2O_2$) in a sealed box of $41.45 \times 41.21 \times 41.25$ Å$^3$, as shown in Fig. 1d. In all directions, the periodic boundary condition was adopted in the simulation model to simulate the actual reaction to a certain extent. The simulation model size is sufficient for the chemical reaction between the organic contaminants and the reactive species according to statistical errors in the data of chemical bonds in the reaction products. Among them, the dissociation
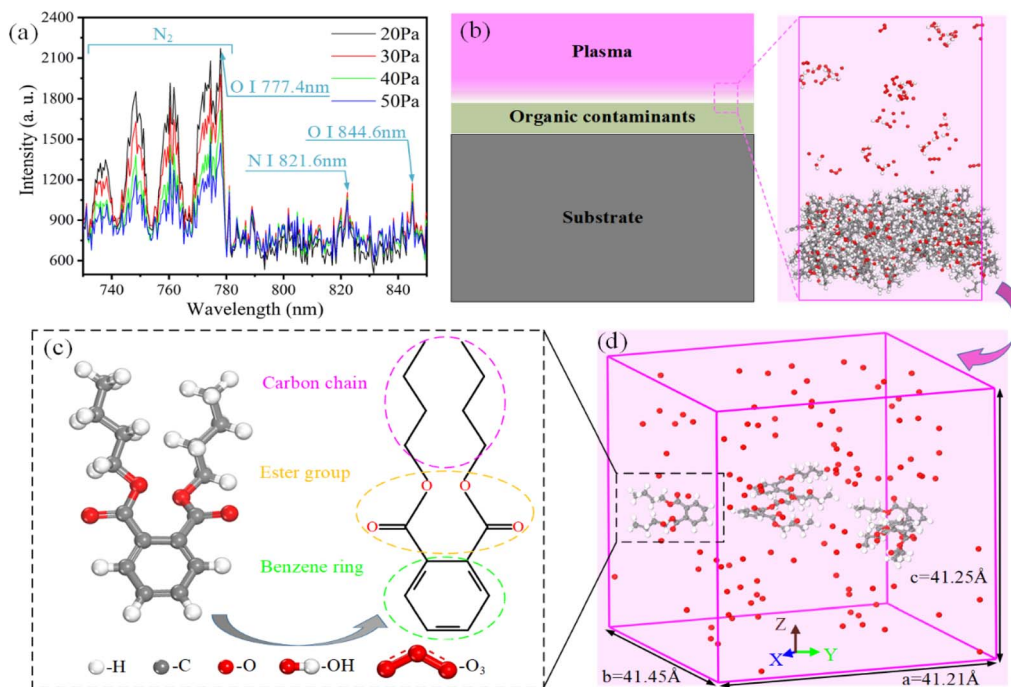
**Fig. 1** Plasma cleaning model and OES spectra: (a) OES spectra of low-pressure air plasma; (b) diagram of plasma cleaning model and the microscopic interface between the plasma and organic contaminants; (c) molecular and chemical structure of DBP; (d) the chemical reaction model between DBP and atomic oxygen was established as a representative of plasma cleaning model.

reactions caused by hydrogen peroxide and superoxide occur because the oxygen atoms in the contaminants capture the hydrogen atoms of these two free radicals.[36] These two radicals also show weak reactive in the molecular interaction and contribute less to the dissociation of contaminants molecules. Therefore, only O, OH and $O_3$ in reactive oxygen reactive species were selected as the objects to study the plasma cleaning mechanism. All the particles were randomly distributed in the box with random velocities. Plasma cleaning models with different reactive species concentrations were performed in an ambient vacuum. Although the plasma concentration exceeds the actual situation,[42] the setting of the reactive species concentrations is acceptable considering the chemical reaction efficiency.[36–39] Besides, according to the experimental temperature range of 298 K to 523 K, we performed isothermal plasma cleaning simulations at 300 K to 800 K to explore the influence of temperature evolution on plasma cleaning characteristics. To speed up the chemical reaction process, relatively high temperatures were selected to study the reaction mechanism. Zhang et al.[43] studied the mechanism of oxidative degradation of organics in supercritical water from 1900 K to 2700 K. They considered that the increase in temperature affected the distribution of products but had no effect on the reaction process.

### 2.2 ReaxFF and simulation parameters

In recent decades, molecular dynamics simulations based on ReaxFF have been developed to describe large-scale complex reaction systems in hydrocarbons while maintaining almost the accuracy based on *ab initio* quantum mechanics.[32] Because

ReaxFF can predict the general bond formation and dissociation process through the general relationship between bond distances, bond orders, and bond energies. Therefore, RMD can show the non-bonding interactions between atoms (including Coulomb force and van der Waals force) and describe the dissociation characteristics of chemical bonds between molecules. The accuracy of ReaxFF in describing reactions between organic molecules and reactive species in plasma has been validated by abundant experiments and simulations.[35–39] In the ReaxFF, the energy of the system is calculated based on the bond order between pairs of atoms, which is divided into various components, as shown in eqn (1):

$$E_{system} = E_{bond} + E_{under} + E_{over} + E_{val} + E_{pen} + E_{tors} + E_{conj} + E_{vdWaals} + E_{Coulomb} \tag{1}$$

where $E_{system}$ is the total energy of the system. $E_{bond}$ denotes the bond order and bond energy. $E_{under}$ and $E_{over}$ are the atom under-/overcoordination as the penalty term of the force field. $E_{val}$, $E_{pen}$, $E_{torsion}$, $E_{conj}$ are the valence angle terms, the penalty energy, the torsion angles, and the conjugated systems, respectively. $E_{valWaals}$ and $E_{Columb}$ represent the nonbonded van der Waals and Coulomb interactions. The detailed energy terms and C/H/O parameters of the ReaxFF force field can be referred to the research of van Duin et al.[32]

In a real electric field excitation environment, abundant reactive oxygen species are generated, which dominate the plasma cleaning process. Due to Auger neutralization, charged reactive oxygen species will capture or lose electrons upon reaching the material surface to achieve charge neutralization.[33]

In addition, neutral radicals have longer lifetimes than charged particles and can sufficiently react with organic contaminants. Therefore, neutral reactive species are used to replace the plasma in the reaction system to perform chemical reactions. This model is widely applied to simulate chemical reactions between plasma and organic molecules.[35–37]

The established simulation model was optimized by energy and geometry under the reactive force field to obtain a more accurate initial reaction model in all MD simulations. The plasma cleaning simulations were performed using the canonical ensemble (*i.e.*, NVT dynamics) with the same number of particles, volume and temperature. The time step and ambient temperature were set to 0.25 fs and 300 K. The Berendsen thermostat was selected to balance the constant temperature throughout the simulation. The result was output every 40 000 steps. Although the total energy of the simulation system does not reach equilibrium, the main chemical reaction of reactive oxygen species with DBP has been completed within 1000 ps. Thus, the simulation is independently executed three times within 1000 ps, considering the consumption of simulation resources, which is also widely accepted in other reactive molecular simulations.[35–37]

## 3 Results and discussions

### 3.1 Data analysis of organic contaminants dissociated by different reactive species concentrations

The cleaning ability of plasma is considered the most important research object for improving cleaning efficiency during practical applications. The mechanism of plasma cleaning is that the reactive species destroy the chemical bonds of organic contaminants and continuously dissociate into small molecular groups. The cleaning ability of reactive species was defined as the ratio of the number of chemical bond cleavage to the total number of chemical bonds of organic contaminants in this work. The cleaning ability of reactive oxygen species was compared under different species concentrations, as shown in Fig. 2a. Generally, the cleaning ability of plasma gradually increases with the increase of oxygen concentration, while the trend of growing cleaning ability is slowing down. The cleaning ability of atomic oxygen and ozone is stronger than that of hydroxyl, and their cleaning ability reaches its highest when the concentration of reactive oxygen is 2.5 nm$^{-3}$. The molecular structure of ozone is unstable, which is easy to decompose into oxygen and atomic oxygen in the plasma environment.[26] The basic process of atomic oxygen, ozone, and carboxyl radical interactions with organic contaminants involves abstracting hydrogen atoms from carbon atoms and further oxidation of C–C bonds. However, both atomic oxygen and ozone can capture twice as hydrogen atoms as hydroxyl,[39] verified by comparing the cleaning ability of reactive oxygen species in Fig. 2a.

On the other hand, the reaction species in plasma are produced by bombarding atoms and molecules with free electrons in the air of gas ionization under an alternating current electric field.[38] These reactive substances gain kinetic energy during elastic collisions with electrons. Although chemical reactions dominate the elimination of organic contaminants in plasma cleaning, physical bombardment may facilitate the reaction process. Thus, we plotted the movement characteristics of reactive species as a function of reaction time in Fig. 2b.
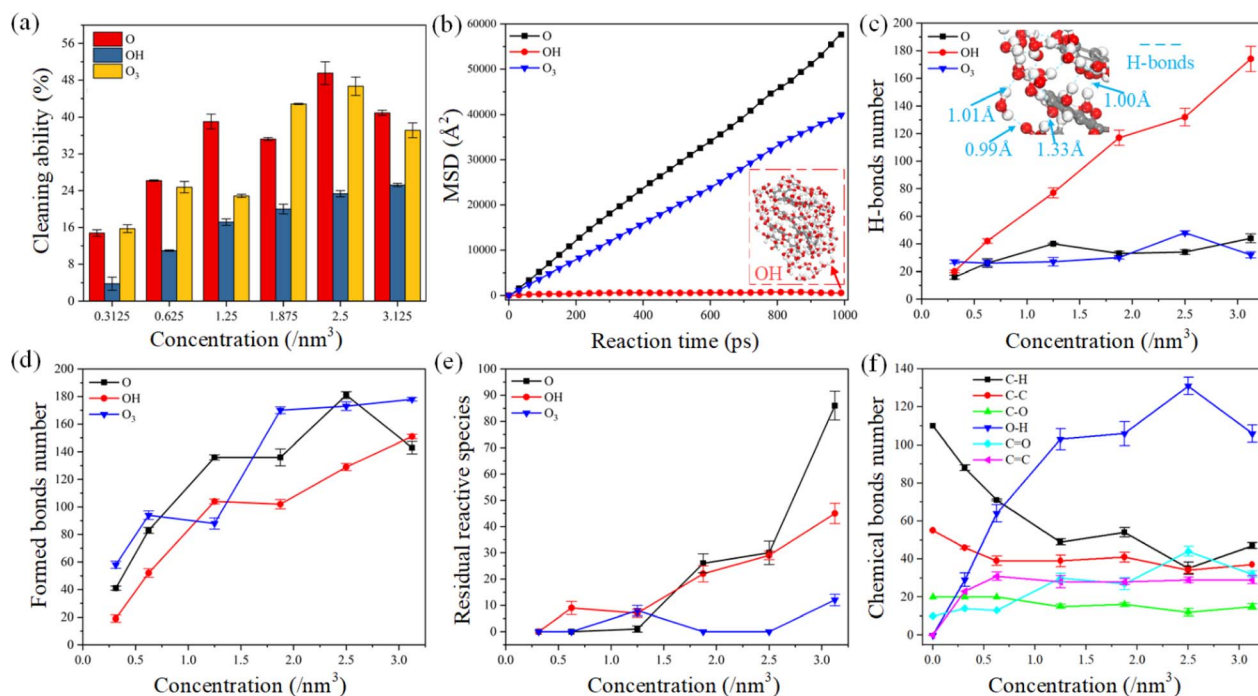


Fig. 2 Statistics of DBP dissociated by different reactive species concentrations: (a) cleaning ability of reactive oxygen species; (b) mobility of reactive species during simulations; (c) hydrogen bonds number; (d) formed bonds number during plasma cleaning; (e) residual reactive species after simulations; (f) chemical bonds number of atomic oxygen.

The mean square displacement (MSD) represents the statistical deviation of the particle position relative to the reference position after moving over time, which can be applied to describe the mobility of the reactive species.[13] The higher the probability of collision and reaction between the reactive species and organic contaminants. The mobility ability of atomic oxygen and ozone is much higher than that of the hydroxyl radical during the chemical reaction, which may be one reason for the stronger cleaning ability of atomic oxygen and ozone. Temporal snapshots show that the hydroxyl radicals cluster together throughout the reaction process, which is attributed to the interaction of hydrogen bonds. Besides, the number of hydrogen bonds formed between hydroxyl radicals and reaction products was calculated according to the hydrogen bond formation rule,[44–46] as shown in Fig. 2c. Compared with atomic oxygen and ozone, abundant hydrogen bonds are generated between the hydroxyl radicals as species concentration increases. The length of hydrogen bonds formed between carboxyl radicals is generally less than 1.5 Å, representing a strong intermolecular interaction.[46] An increase in the number of hydrogen bonds may decrease the cleaning efficiency due to the limited movement of the reactive species.

In plasma cleaning, reactive oxygen destroys chemical bonds in organic contaminants molecules and generates abundant new chemical bonds. Thus, we conducted the statistics of the formed chemical bonds and residual reaction species in the model after simulating 1000 ps, as shown in Fig. 2d and e. The number of formed bonds varies with the concentration in a similar trend to the cleaning ability of the reactive species, suggesting that bond formation and dissociation occur simultaneously. The number of chemical bonds of organic contaminants is proportional to the concentration of reactive oxygen species. When the oxygen concentration exceeds 2.5 nm$^{-3}$, there are abundant residual species in simulation models which are not involved in the chemical reaction. Therefore, controlling the reactive oxygen species in a certain concentration range is economical in the plasma cleaning process.

Furthermore, we investigated the relationship between the evolution of chemical bonds number in detail and the concentration of atomic oxygen, as shown in Fig. 2f. With the increase in reactive species concentration, C–H, C–C and C–O bonds were destroyed. Abundant O–H, C=C and C=O bonds were generated, eventually leading to the molecular structure collapse of organic contaminants. O–H and C=O bonds are the main chemical bonds of water and carbon dioxide molecules, which can be widely detected on the surface of components after plasma cleaning.[1,4,47] The O–H bond generates from the C–H bond cleavage of the DBP molecular structure caused by the hydrogen abstraction reaction of atomic oxygen. The C=C bond is developed between the carbon atoms when the hydrogen is abstracted from carbon atoms. However, the C=C bond has an unstable structure, which is further oxidized by atomic oxygen to form C=O bonds.

After simulations, the evolution of chemical bond number percentage with different reactive species and their concentration are compared in Fig. 3. The error bars were deleted to visualize the percentage of chemical bonds in simulations

directly. Only the bonds involved in chemical reactions and DBP bonds were calculated here. The percentage of bonds in the product of the reaction between the hydroxyl functional radical and DBP is very sensitive to the concentration of the reacting species compared to atomic oxygen and ozone. The O–H bond percentage increases significantly with the increased hydroxyl concentration, while C–C and C–H bond percentages decrease sharply. The percentage decline in the number of C–C and C–H bonds is partly due to breaking these bonds but more to the formation of abundant O–H bonds.

According to the above analysis of the mobility of hydroxyl radicals, the increase of O–H will lead to the formation of abundant hydrogen bonds between atoms, resulting in the decline of reaction efficiency. On the contrary, the percentage of reaction products of atomic oxygen and ozone with organic contaminants shows a similar trend. As the concentration of the reaction increases, the number of bonds changes dramatically and then tends to plateau. The number of O–H, C–H and C–C bonds changed significantly among them. Atomic oxygen reacts with hydrogen atoms on C–H to form O–H. Besides, the generated O–H bonds can also develop new O–H bonds with other atomic oxygen. The increased concentration of reactive species also promotes the efficiency of chemical reactions. The C–C and C–O bonds are gradually oxidized to C=C and C=O bonds. But we can find that even though the chemical reaction is complete at a concentration of 3.125 nm$^{-3}$, the C–H bond and C–C bond still account for a very high proportion of the reaction products and are not involved in the reaction. Because the benzene ring in DBP has the delocalized π bond, which is quite stable. The C–H and C–C bonds on the benzene ring are hard to be broken during the whole reaction process, as shown in Fig. 3d. The C–O bond between the carbon chain and the ester radical on the side chain of the benzene ring is broken first. As the chemical reaction progresses, the carbon chain gradually breaks into small molecular radicals composed of O–H, C=O and C–O bonds. In the reaction process of atomic oxygen and DBP at 300 K, the system's total energy is consistent with the evolution trend of atomic oxygen concentration. These results further confirm that the concentration of reactive species determines the chemical reaction efficiency in the plasma cleaning process.

### 3.2 Evolution characteristics of key chemical bonds in DBP

The detailed evolution of key chemical bonds during the reaction process is helpful to the understanding of the plasma cleaning process, as shown in Fig. 4. OH has the weakest cleaning ability and induces the least hydrogen abstraction reaction. Therefore, under the trigger of OH radicals, the number of C–H, C–C and C–O bonds in DBP decreases the most, while the number of C=O and C=C bonds is the least. The evolutions in C–C, C–O, O–H and C=C bond numbers of atomic oxygen and ozone radicals are not obvious compared with those of hydroxyl radicals, indicating the cleavage of the C–H bond and the formation of the C=O bond of atomic oxygen and ozone have significant contributions. The number of bonds in the reaction varies dramatically during the first 400 ps, after
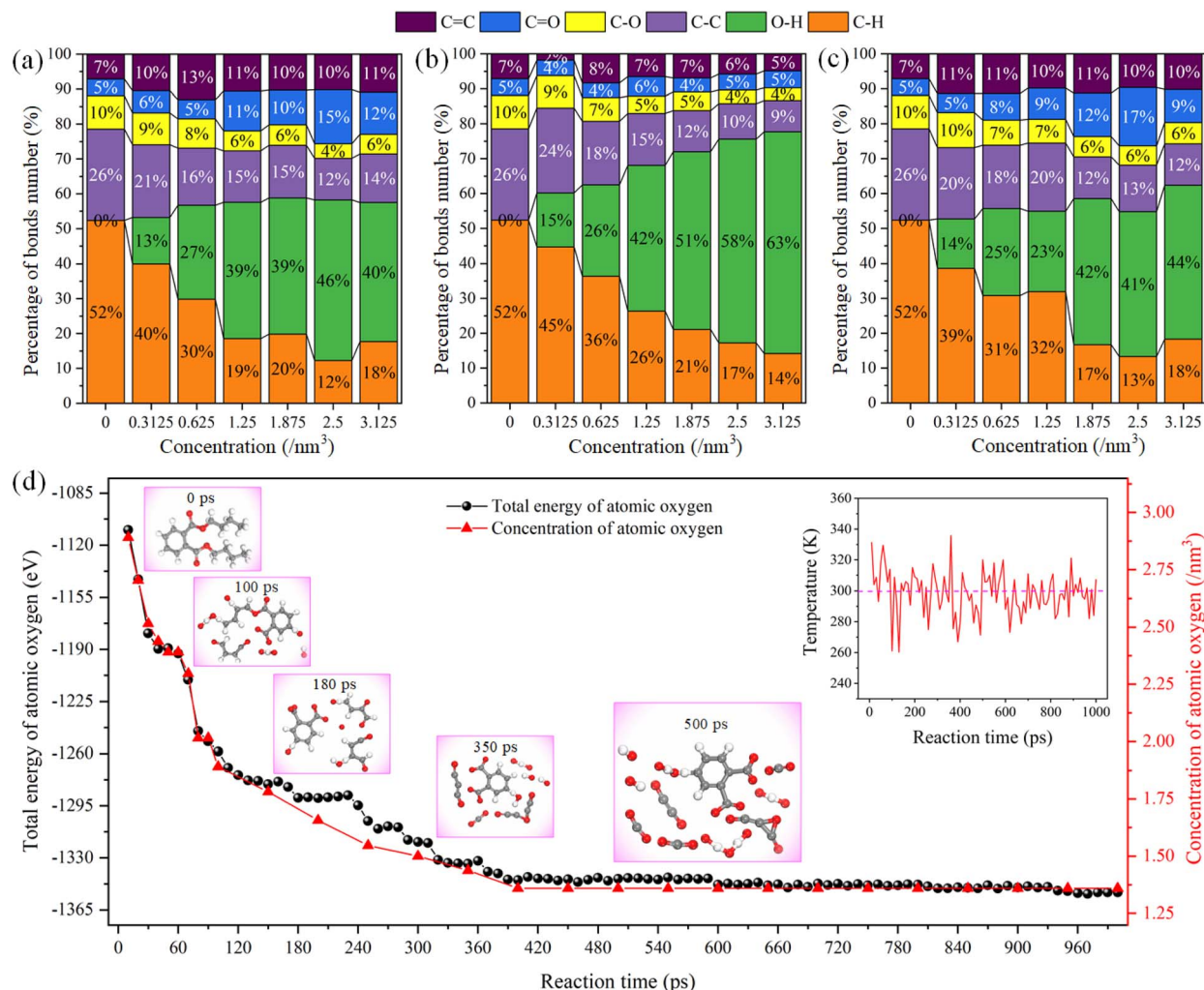
Fig. 3 Evolution behaviors of chemical bonds percentage in simulations with varying reactive species (a) O, (b) OH and (c) $O_3$ and their concentration. (d) Evolution of total energy and species concentration in atomic oxygen reaction systems during 1000 ps.

which the reaction gradually stops as the concentration of the reacting species decrease.

According to the above simulation results, C–H bond breaking and C=C, C–O and C=O bond formation are the main characteristics of chemical reactions during plasma cleaning, revealed by real-time atom trajectories in Fig. 5. Fig. 5a shows the real-time trajectory of atomic oxygen abstracting a hydrogen atom from a methyl radical. The atomic oxygen interacts more strongly with the hydrogen in the methyl radical, and the distance is shorter along with the reaction time. C–H is broken by atomic oxygen and forms the O–H bond at 3.28 ps. Similarly, the hydrogen atoms of ethyl on the DBP branch are abstracted away by the atomic oxygen, as shown in Fig. 5b. Since the carbon atom on the methyl radical is also losing a hydrogen atom, the carbon atom on the methyl radical and the carbon atom on the ethyl radical form a C=C bond at 7.10 ps, which is unstable and will be further oxidized to a C=O bond. However, the carbon atom on the ethyl radical will be further oxidized to a C–O bond at 1.20 ps when the ethyl radical loses a hydrogen

atom. The methyl radical does not lose hydrogen atoms in Fig. 5c. If the ethyl hydrogen next to the methyl is not abstracted. Hydrogen is lost from the methyl, and the methyl is easily oxidized to form a C–O bond. At the same time, since the C–O bond is at the end of the carbon chain, the C–C bond tends to dissociate and form a C=O bond at 7.20 ps. Therefore, the cleavage of C–H in the reaction process of plasma cleaning is the basis of the reaction, and further oxidation can produce the bonds of C=C, C–O and C=O.

### 3.3 Influence of ambient temperature on the evolution of the chemical bond during plasma cleaning

Fig. 6 illustrates the interaction characteristics and simulated data statistics of reactive oxygen species and DBP with different ambient temperatures. The cleaning ability of reactive oxygen species increased gradually with the increase in ambient temperature, as shown in Fig. 6a. The cleaning ability of hydroxyl radical was significantly improved because the temperature rise reduced the aggregation of O–H and increased
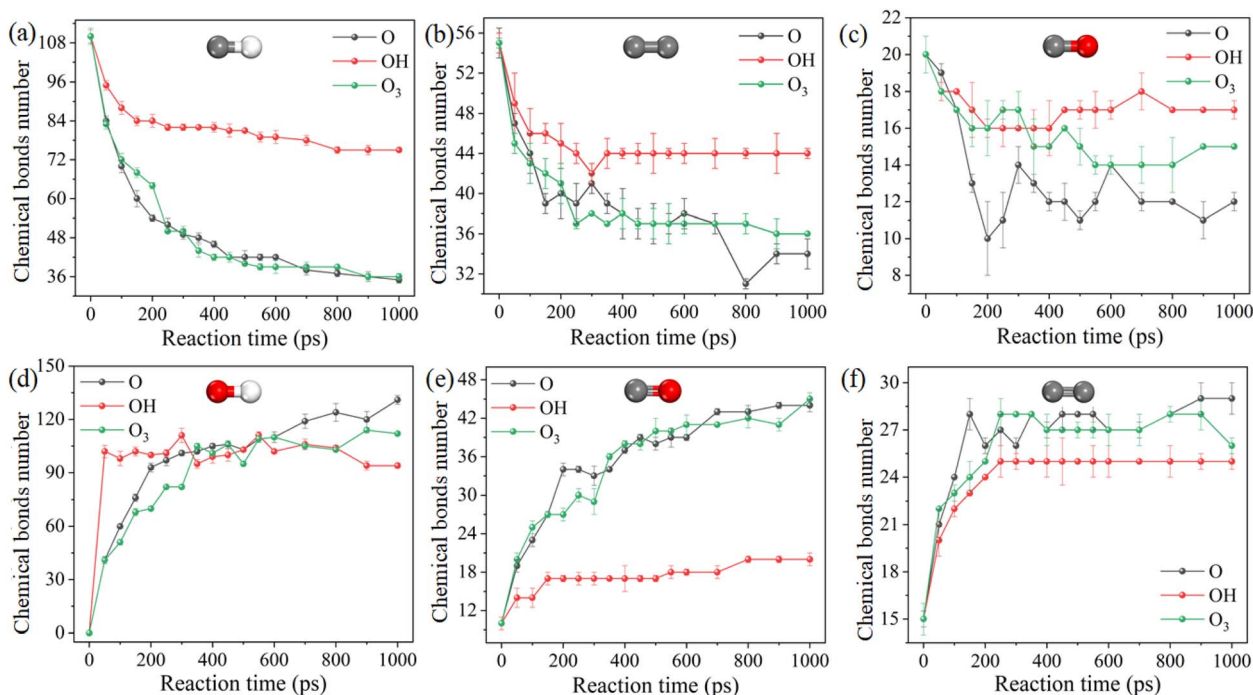
**Fig. 4** Evolution behaviors of key chemical bonds during chemical reactions with 3.125 nm$^{-3}$ at 300 K. (a–f): C–H, C–C, C–O, O–H, C=O, C=C.



**Fig. 5** Temporal snapshots of (a) C–H bond dissociation and O–H bond formation, (b) C–C bond dissociation and C=C formation, (c) C–O and (d) C=O bond formation mechanism induced by atomic oxygen. The hydrogen atom is abstracted by oxygen atoms, leading to the destruction of C–H bonds and the formation of O–H, C=C, C–O, and C=O. Dotted lines indicate the distance between atoms.

the effective intermolecular collision, which consistent with the research of Samaei *et al.*[30] On the contrary, the cleaning ability of atomic oxygen and ozone molecular radicals remains unchanged when the temperature exceeds 600 K, which indicates reactive species sufficiently react with DBP molecules. At the same concentration of reactive species (1.875 nm$^{-3}$), the increasing temperature cannot further improve the cleaning ability of reactive species. Similar results could be obtained in Fig. 6b. Through the total energy of the simulation system does not reach the equilibrium, the main chemical reaction of reactive oxygen species with DBP has been completed within 1000 ps. It can be found that the increase of ambient temperature has little influence on the decreasing trend of total energy in the system reaction process when the system temperature exceeds 600 K. Fig. 6c shows that the mobility of molecules in the system is significantly improved after the temperature exceeds 600 K. Although the increase in temperature can promote the frequency of intermolecular collision, the growth of intermolecular collision does not contribute significantly to the improvement of cleaning ability when the reaction is sufficient.

Furthermore, we calculated the percentage distribution of chemical bonds in the reaction system as the temperature increased in Fig. 6d–f, which directly shows ambient temperature's influence on the reaction products. With the increase in ambient temperature, the proportion of C–H, O–H and C=C bonds in the reaction products decreased gradually. The temperature rise promoted the mobility of the reactive species, and the reaction with organic contaminants was adequate. The C–H, C–C, and C=C bonds were further oxidized to C–O and C=O bonds. Besides, the increase in kinetic energy of the reactive species overcomes the aggregation of O–H through hydrogen bonds.
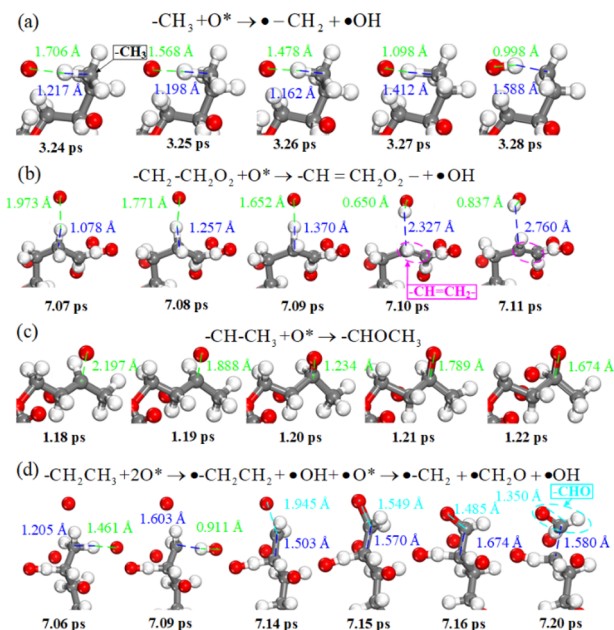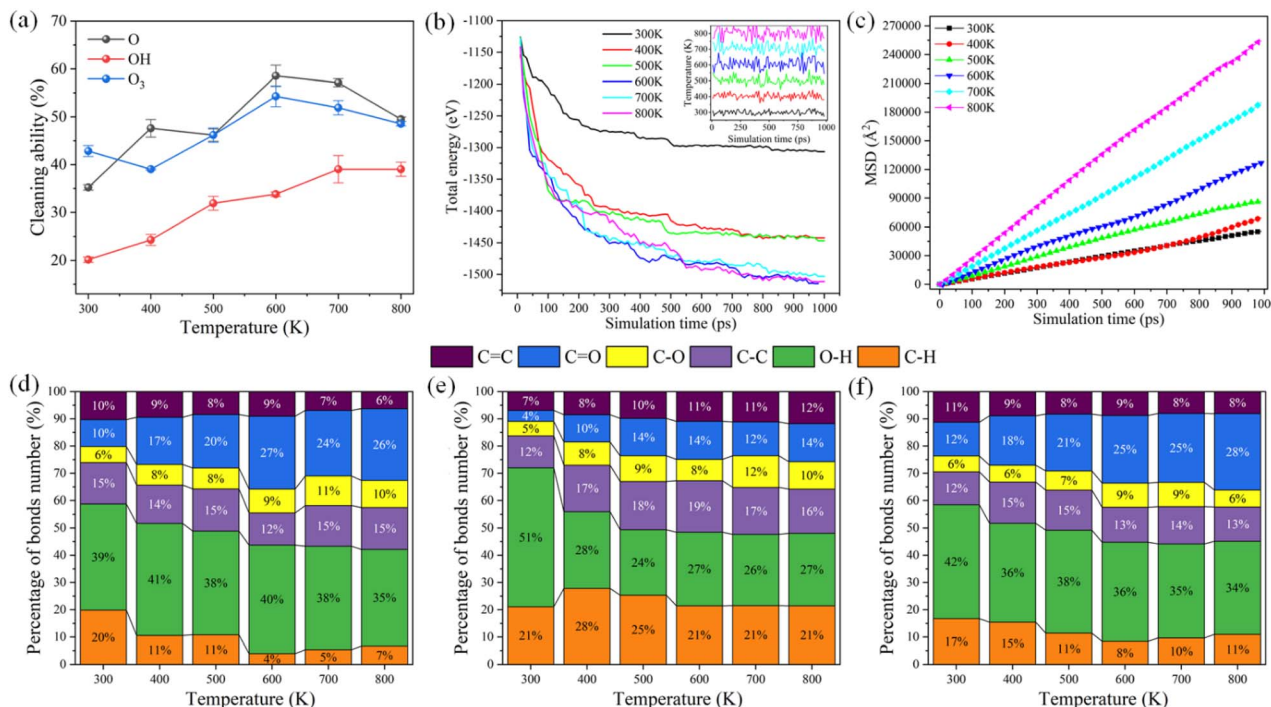
**Fig. 6** Statistics of DBP dissociated by different reactive species under various ambient temperatures: (a) cleaning ability of reactive oxygen species; (b) evolution of total energy in atomic oxygen reaction systems; (c) mobility of atomic oxygen during simulations. Evolution behaviors of chemical bonds percentage in simulations with varying reactive species (d) O, (e) OH, (f) O$_3$ and ambient temperatures.

When the concentration of the reaction species reaches a certain concentration, the increase in temperature will further improve the plasma cleaning ability. This means that more chemical bonds (such as C–H and C–C) are oxidized to C=C, C–O, C=O, and O–H *via* hydrogen abstraction reactions. In particular, the molecular structure of the benzene ring, which is difficult to decompose in the experiment,[29] can be destroyed by increasing the temperature. The carbon ring structure of the benzene ring is very stable and is not easily replaced and oxidized. However, the benzene ring is gradually broken with ambient temperature increase during the plasma cleaning process.

The detailed microscopic destruction pathway can be described in Fig. 7. First, the atomic oxygen gradually approaches the hydrogen atom on the benzene ring and forms an O–H bond. The H–O bond on the benzene ring further exchanged positions to form the phenol structure after
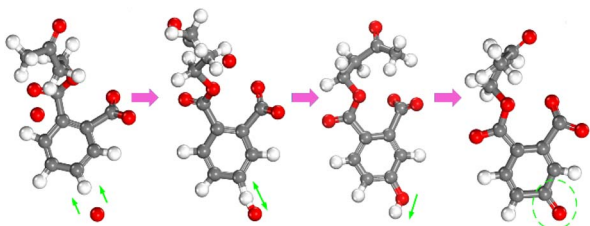
molecular structure equilibrium. In phenol molecular structure, the polarity of the O–H bond was strengthened by the action of the delocalized π bond. Therefore, hydrogen atoms in the hydroxyl radical of phenol are easily ionized to form a C=O structure. After the delocalized π bond of the benzene ring is destroyed, DBP molecular structure will be gradually decomposed into small molecular groups. In all simulations, this pathway of the benzene ring is widely found in the interaction between reactive species and the benzene ring in a high-temperature environment.

## 4 Conclusions

In this work, ReaxFF molecular dynamics simulations were proposed to study the microscopic cleaning mechanism of the reaction between organic contaminants and reactive oxygen species in plasma at the atomic level. We elucidated the effects of reactive oxygen species concentration and ambient temperature on plasma cleaning characteristics. The evolution characteristics of chemical bonds in the plasma cleaning process were revealed. In the plasma cleaning process, hydrogen abstraction reaction dominated the chemical reaction between reactive oxygen species and organic contaminants. The cleaning ability of the atomic oxygen and ozone radical was the strongest among the studied reactive oxygen species in the plasma. The reason can be attributed to the mobility of the atomic oxygen and ozone radical, which is much higher than that of the hydroxyl radical. The formation of abundant hydrogen bonds between hydroxyl radicals led to aggregation and reduced the



**Fig. 7** The microscopic pathway of the benzene ring is destroyed by atomic oxygen in DBP molecules.

efficiency of chemical reactions. As the reaction duration, C–H, C–C and C–O bonds in organic contaminants molecules were gradually oxidized into O–H, C=C and C=O bonds. In a certain range of reactive oxygen species concentration, the cleaning ability of plasma increased gradually with the increase of atomic oxygen concentration. When the concentration of reactive oxygen species was 2.5 $nm^{-3}$, the cleaning ability reached the highest. At the same time, the probability of C–H, C–C and C–O bonds being destroyed to form abundant O–H, C=C and C=O bonds gradually increased with the rise of the concentration of reactive species. The cleavage reaction of the C–H bond was the basis of the chemical reaction in the plasma cleaning process. With the increase in ambient temperature, the cleaning ability of reactive oxygen species in plasma was further improved, and the proportion of the O–H bond, C–H bond and C=C bond in reaction products decreased gradually. Reactive oxygen species gained more kinetic energy in a high-temperature environment, promoted reaction efficiency with organic contaminants, and overcame O–H aggregation. The benzene ring structure, which was difficult to decompose at room temperature, could be destroyed by raising the ambient temperature.

## Author contributions

Yuhai Li: conceptualization, data curation, formal analysis, investigation, methodology, resources, software, writing – original draft, writing – review & editing. Yilan Jiang: conceptualization, data curation, formal analysis, investigation, methodology, resources. Xujie Liu: conceptualization, data curation, formal analysis, investigation, methodology. Qingshun Bai: funding acquisition, conceptualization, investigation, methodology, resources, validation. Hao Liu: data curation, formal analysis, investigation, methodology. Jingxuan Wang: conceptualization, investigation, methodology, resources. Peng Zhang: funding acquisition, project administration, resources. Lihua Lu: project administration, resources. Xiaodong Yuan: methodology.

## Conflicts of interest

There are no conflicts to declare.

## Acknowledgements

## References

1 L. Bónová, A. Zahoranová, D. Kováčik, M. Zahoran, M. Mičušík and M. Černákab, *Appl. Surf. Sci.*, 2015, **79**, 331.

2 M. Boselli, C. Chiavari, V. Colombo, M. Gherardi, C. Martini and F. Rotundo, *Plasma Processes Polym.*, 2017, **14**, 1600027.

3 A. Zille, F. R. Oliveira and A. P. Souto, *Plasma Processes Polym.*, 2015, **12**, 98.

4 Y. Li, Q. Bai, Y. Guan, P. Zhang, R. Shen, L. Lu, H. Liu, X. Yuan, X. Miao, W. Han and C. Yao, *Nucl. Fusion*, 2022, **62**, 076023.

5 J. A. Pryatel, W. H. Gourdin, S. C. Frieders, G. S. Ruble and M. V. Monticelli, *Laser-Induced Damage in Optical Materials: 2014*, 2014, vol. 9237, p. 92372H.

6 H. P. Howard, A. F. Aiello, J. G. Dressler, N. R. Edwards, T. J. Kessler, A. A. Kozlov, I. R. T. Manwaring, K. L. Marshall, J. B. Oliver, S. Papernov, A. L. Rigatti, A. N. Roux, A. W. Schmid, N. P. Slaney, C. C. Smith, B. N. Taylor and S. D. Jacobs, *Appl. Optics*, 2013, **52**, 1682–1692.

7 J. R. Vig, *J. Vac. Sci. Technol., A*, 1985, **3**, 1027.

8 Y. Ye, X. Yuan, X. Xiang, X. Cheng and X. Miao, *Optik*, 2012, **123**, 1056.

9 L. Huang, H. Yan, L. Yan, T. Liu, Z. Zhang, K. Yang, C. Li and Y. Qian, *J. Sol-Gel Sci. Technol*, 2022, **101**, 630.

10 L. Petersson, P. Meier, X. Kornmann and H. Hillborg, *J. Phys. D: Appl. Phys.*, 2010, **44**, 034011.

11 D. F. O'Kane and K. L. Mittal, *J. Vac. Sci. Technol.*, 1974, **11**, 0567.

12 T. C. Isabell, P. E. Fischione, C. O'Keefe, M. U. Guruz and V. P. Dravid, *Microsc. Microanal.*, 1999, **5**, 126.

13 Y. Li, Q. Bai, C. Yao, P. Zhang, R. Shen, H. Liu, L. Lu, Y. Jiang, X. Yuan, X. Miao and W. Han, *Appl. Surf. Sci.*, 2021, **581**, 152358.

14 W. Petasch, B. Kegel, H. Schmid, K. Lendenmann and H. U. Kellerb, *Surf. Coat. Technol.*, 1997, **97**, 176.

15 R. Yan, L. Moser, B. G. Wang, J. Peng, C. Vorpahl, F. Leipold, R. Reichle, R. Ding, J. L. Chen, L. Mu, R. Steiner, E. Meyer, M. Z. Zhao, J. H. Wu and L. Maro, *Nucl. Fusion*, 2017, **58**, 026008.

16 M. J. Shenton, M. C. Lovell-Hoare and G. C. Stevens, *J. Phys. D: Appl. Phys.*, 2001, **34**, 2754.

17 D. P. R. Thanu, E. S. Srinadhu, M. R. Zhao, N. V. Dole and M. Keswani, *Developments in Surface Contamination and Cleaning: Applications of Cleaning Techniques*, Elsevier Inc., Tucson, 2019, pp. 289–353.

18 C. L. Hyoun, W. Kim and S. Kim, *Appl. Surf. Sci.*, 2007, **253**, 3658.

19 S. Kelly and M. M Turner, *Plasma Sources Sci. Technol.*, 2014, **23**, 065013.

20 R. Ono, *J. Phys. D: Appl. Phys.*, 2016, **49**, 083001.

21 T. Takamatsu, K. Uehara, Y. Sasaki, H. Miyahara, Y. Matsumura, A. Iwasawa, N. Ito, T. Azuma, M. Kohnoc and A. Okinoa, *RSC Adv.*, 2014, **4**, 39901.

22 J. M. Grace and L. J. Gerenser, *Sci. Technol.*, 2003, **24**, 305.

23 D. Marinov, J. F. Marneffe, Q. Smets, G. Arutchelvan, K. M. Bal, E. Voronina, T. Rakhimova, Y. Mankelevich, S. E. Kazzi, A. N. Mehta, P. J. Wyndaele, M. H. Heyne, J. R. Zhang, P. C. With, S. Banerjee, E. C. Neyts, I. Asselberghs and D. L. S. D. Gendt, *npj 2D Mater. Appl.*, 2021, **5**, 1.

24 D. Ferrah, O. Renault, D. Marinov, J. Arias-Zapata, N. Chevalier, D. Mariolle, D. Rouchon, H. Okuno,

© 2022 The Author(s). Published by the Royal Society of Chemistry

V. Bouchiat and G. Cunge, *ACS Appl. Nano Mater.*, 2019, **2**, 1356.

25 F. Normand, A. Granier, P. Leprince, J. Marec and M. K. S. F. Clouet, *Plasma Chem. Plasma Process.*, 1995, **15**, 173.

26 S. Park, W. Choe and C. Joc, *Chem. Eng. J.*, 2018, **352**, 1014.

27 M. Mafra, T. Belmonte, F. Poncin-Epaillard, A. S. da Silva Sobrinho and A. Maliska, *Plasma Chem. Plasma Process.*, 2008, **28**, 495.

28 E. A. Bernardelli, T. Belmonte, D. Duday, G. Frache, F. Poncin-Epaillard, C. Noël, P. Choquet, H.-N. Migeon and A. Maliska, *Plasma Chem. Plasma Process.*, 2011, **31**, 189.

29 R. R. A. Callahan, G. B. Raupp and S. P. Beaudoin, *J. Vac. Sci. Technol., B*, 2001, **19**, 725.

30 A. Samaei and S. Chaudhuri, *J. Appl. Phys.*, 2020, **128**, 054903.

31 B. Li, M. Chen, J. Liu and S. Xue, *Vacuum*, 2019, **163**, 135.

32 A. C. T. van Duin, S. Dasgupta, F. Lorant and W. A. Goddard, *J. Phys. Chem. A*, 2001, **105**, 9396.

33 H. D. Hagstrum, *Phys. Rev.*, 1961, **122**, 83.

34 Y. Han, D. D. Jiang, J. L. Zhang, W. Li, Z. X. Gan and J. J. Gu, *Front. Chem. Sci. Eng.*, 2016, **10**, 16.

35 Y. Lv, L. Zou, H. D. Li, Z. L. Chen, X. L. Wang, Y. Sun, L. P. Fang, T. Zhao and Y. T. Zhang, *Plasma Sci. Technol.*, 2021, **23**, 055506.

36 J. Cui, T. Zhao, L. Zou, X. Wang and Y. Zhang, *J. Phys. D: Appl. Phys.*, 2018, **51**, 355401.

37 S. Tian, X. Wang and Y. Zhang, *Plasma Processes Polym.*, 2021, **18**, 2100124.

38 Y. Li, Q. Bai, Y. Guan, H. Liu, P. Zhang, B. Batelibieke, R. Shen, L. Lu, X. Yuan, X. Miao, W. Han and C. Yao, *Plasma Sci. Technol.*, 2022, **24**, 064012.

39 T. Zhao, L. Shi, Y. T. Zhang, L. Zou and L. Zhang, *Phys. Plasmas*, 2017, **24**, 103518.

40 T. Belmonte, C. Noël, T. Gries, J. L. Martin and G. Henrion, *Plasma Sources Sci. Technol.*, 2015, **24**, 064003.

41 K. R. Manes, M. L. Spaeth, J. J. Adams, M. W. Bowers, J. D. Bude, C. W. Carr, A. D. Conder, D. A. Cross, S. G. Demos, J. M. G. D. Nicola, S. N. Dixit, E. Feigenbaum, R. G. Finucane, G. M. Guss, M. A. Henesian, J. Honig, D. H. Kalantar, L. M. Kegelmeyer, Z. M. Liao, B. J. MacGowan, M. J. Matthews, K. P. McCandless, N. C. Mehta, P. E. Miller, R. A. Negres, M. A. Norton, M. C. Nostrand, C. D. Orth, R. A. Sacks, M. J. Shaw, L. R. Siegel, C. J. Stolz, T. I. Suratwala, J. B. Trenholme, P. J. Wegner, P. K. Whitman, C. C. Widmayer and S. T. Yang, *Fusion Sci. Technol.*, 2016, **69**, 146.

42 T. Verreycken, R. Mensink, R. van der Horst, N. Sadeghi and P. J. Bruggeman, *Plasma Sources Sci. Technol.*, 2013, **22**, 055014.

43 J. L. Zhang, J. T. Gu, Y. Han, W. Li, Z. X. Gan and J. J. Gu, *J. Mol. Model.*, 2015, **21**, 1.

44 I. Y. Torshin, I. T. Weber and R. W. Harrison, *Protein Eng., Des. Sel.*, 2002, **15**, 359.

45 I. Alkorta, I. Rozas and J. Elguero, *Chem. Soc. Rev.*, 1998, **27**, 163.

46 A. Vedan, *J. Comput. Chem.*, 1988, **9**, 269.

47 D. Li, M. Xiong, S. Wang, X. Chen, S. Wang and Q. Zeng, *Appl. Surf. Sci.*, 2020, **503**, 144257.